JOURNAL OF CATALYSIS 92, 25–34 (1985)

Reaction Kinetic Measurements on Single Crystal Catalysts: Methanol Decomposition on Ni(111)

S. M. GATES, J. N. RUSSELL, JR., AND J. T. YATES, JR.

Surface Science Center, Department of Chemistry, University of Pittsburgh, Pittsburgh, Pennsylvania 15260

Received September 18, 1984; accepted October 5, 1984

A simple apparatus and methodology are presented for reaction kinetic measurements over clean single crystal catalysts in ultrahigh vacuum. Three useful quantities are simultaneously measured in one isothermal experiment: (1) steady-state reaction rate constant (f^R_{SS}), (2) surface coverage of stable intermediates at steady state (θ_{SS}(CO), θ_{SS}(H)), and (3) zero coverage reactive sticking coefficient (S^R_0) of the reactant. The decomposition of methanol to CO(g) and H_2(g) on Ni(111) is used as a model reaction. The observed dependence of steady-state decomposition rate on temperature is modeled using S^R_0(T) and the fraction of empty surface sites. This "site blocking" model qualitatively fits the reaction kinetics from 300 to 500 K. Previously, measurements of S^R_0 revealed a deuterium kinetic isotope effect (KIE) in the reaction of methanol with a clean Ni(111) surface (S. M. Gates, J. N. Russell, Jr., and J. T. Yates, Jr., *Surface Sci.* **146,** 199 (1984). CH_3OH and CD_3OH are 1.5 times more reactive at zero coverage than CH_3OD (300–400 K). This observation is now extended to steady-state reaction conditions (SS). The ratio f^R_{SS} (O–H)/f^R_{SS} (O–D) has a maximum value of 2.2 at 363 K and decreases monotonically to about 1 at 500 K. The kinetic isotope effect is also observed from measurements of θ_{SS}(CO), the steady-state CO surface coverage. Addition of products (CO or H_2) to the steady-state reaction *decreases* the decomposition rate by *decreasing* the number of empty surface sites.

I. INTRODUCTION

Current interest in the use of single crystal surfaces as model catalytic systems is related to the unique opportunity this approach provides for control of many factors of importance in determining the kinetics of catalytic reactions (*2–6*). Among the factors which enhance the single crystal approach are

(1) control of surface crystallography,

(2) absence of surface impurities,

(3) absence of catalytic support effects,

(4) absence of heat and mass transport effects, and

(5) ability to make physical measurements closely related to the elementary processes at work on the surface.

For single crystal metal surfaces, this approach affords an opportunity to view the *inherent catalytic behavior of the metal,* and may form a sound basis for understanding more complex catalytic surfaces of technological importance.

We have selected the reaction

$$CH_3OH(g) + Ni(111) \xrightarrow{S^R_0} CH_3O(ads) + H(ads) \rightarrow CO(g) + 2H_2(g) \quad (1)$$

for detailed study. It will be shown that the use of a simple apparatus involving a molecular beam of reactant incident on a metal single crystal, combined with mass spectrometric detection of reactant consumption and product evolution, can effectively be used to dissect certain elementary steps controlling the catalytic process. This capability is enhanced by the use of deuterium labeling at specific sites within the reactant molecule to gain insight into the details of bonding and molecular fragmentation which occur during the reaction.

II. EXPERIMENTAL

The UHV apparatus shown in Fig. 1 has been described elsewhere (*1*) and only a brief description of its operation will be given here. The Ni(111) single crystal was

0021-9517/85 $3.00

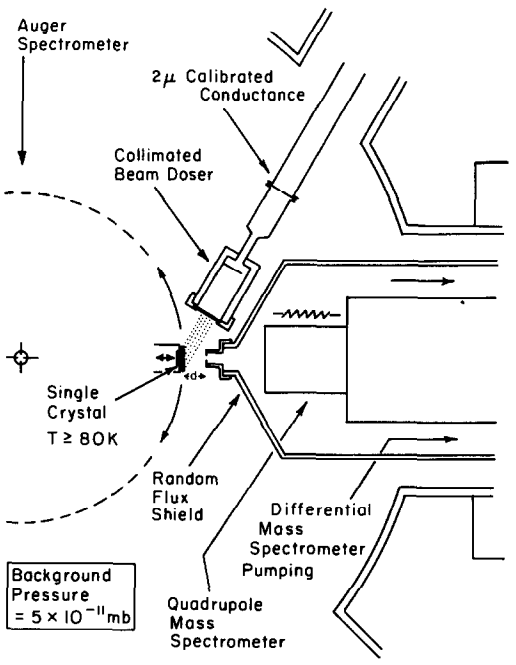

FIG. 1. Top view of the UHV apparatus constructed for study of surface reaction kinetics on single crystal surfaces.

mounted on 0.5-mm-diameter W leads by welding. It was cleaned by cycles of Ar^+ bombardment, followed by heating to 1050 K. No surface impurities were detected by Auger electron spectroscopy following this cleaning procedure. A known flux collimated molecular beam of methanol is directed into the vacuum system, and at time = 0, the atomically clean Ni(111) single crystal (at constant temperature) is rotated into the beam. Desorption of product molecules and reflection/desorption of reactant methanol can be monitored by means of a closely coupled multiplexed quadrupole mass spectrometer which is present inside a random flux shield, differentially pumped by a 60-l/sec ion pump.

Typical data are shown in Fig. 2. At a stable background pressure of methanol, P_1, rotation of the clean Ni(111) crystal into the beam results in an *immediate* rise in methanol signal to P_2. Eventually the reflected methanol signal reaches the steady-state value, P_3. Verification of the steady-state condition is described below. P_4 is a reference methanol mass spectrometer signal corresponding to 100% reflection of the incident beam. The pressure change ($P_4 - P_1$) represents 100% reflection of the methanol beam and has been discussed previously (*1*).

The upper panels of Fig. 2 illustrate the evolution of D_2 due to CH_3OD(left) and CD_3OH(right) catalytic decomposition on Ni(111) plotted versus time. When the crys-

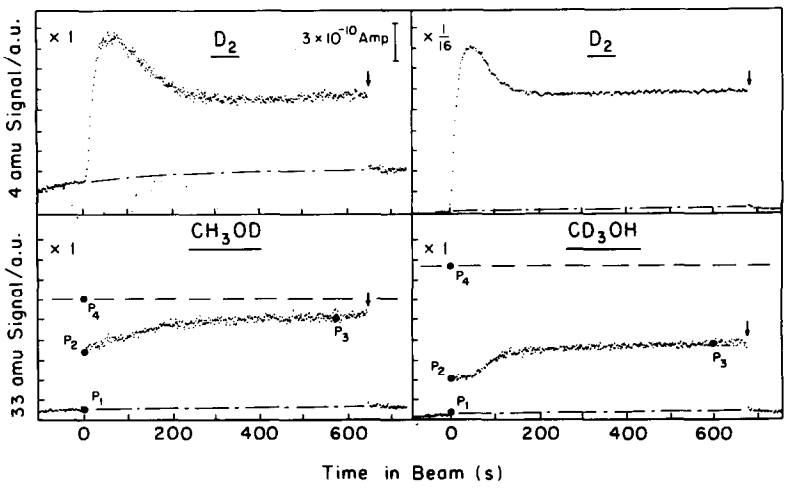

FIG. 2. Representative data showing isothermal decomposition of CH_3OD (left) and CD_3OH (right) on Ni(111) at 351 K. Zero time and vertical arrow show rotation of crystal in and out of methanol beam, respectively. Pressures P_1, P_2, P_3, and P_4 are explained in the text.

tal is rotated to the in-beam position, the D_2 signal first increases, then decreases, and then stabilizes as the surface coverage of H, D, and CO approach the steady-state condition coverages.

The steady-state condition of the catalytic surface in the beam is verified by monitoring at various times the CO coverage using temperature programmed desorption. This is done by ramping the crystal temperature (dT/dt = 2 K/s) after point P_3 in the isothermal experiment (see Fig. 2), without moving the crystal or turning off the beam. Representative data are shown in Fig. 6.

The CO desorption peak areas so obtained (see Fig. 6) are expressed relative to a CO desorption area obtained from a saturation coverage of pure CO on Ni(111) at 300 K. This CO coverage has been shown (*7, 8*) to give a sharp c[4 × 2] LEED pattern on Ni(111) corresponding to an absolute coverage of θ = 0.5 CO/Ni atom. All θ(CO) values reported here are expressed relative to the number of nickel atoms on the Ni(111) surface, 1.86×10^{15} cm^{-2}.

When ramping the crystal temperature, the D_2 thermal desorption peak area is also monitored to determine the *relative* steady-state deuterium coverage, n_{SS}(D). Unlike θ(CO), n_{SS}(D) is not calibrated to an absolute D coverage; the D_2 desorption peak areas are expressed *relative* to the maximum desorption *area* measured (steady state at 250 K).

Auger studies following all methanol experiments in which the crystal was heated beyond the CO desorption temperature have shown that residual surface carbon is not left behind on the Ni(111) surface.

III. RESULTS

A. *Reflected Methanol Measurements*

Kinetic measurements for the isothermal decomposition rate of CH_3OH, CD_3OH, and CH_3OD have been made throughout the temperature range 200 to 500 K on Ni(111). It will be shown that CH_3OD is consistently *less reactive* on Ni(111) than either CH_3OH or CD_3OH for clean, transient and steady-state surface conditions, respectively. Representative data used to determine the methanol decomposition rate under various conditions are shown in Fig. 2.

A deuterium kinetic isotope effect was previously reported (*1*) for methanol isothermal decomposition on clean Ni(111) using measurements of the reactive sticking coefficient, S_0^R, under zero coverage (completely irreversible) conditions. The zero coverage reactive sticking coefficient, S_0^R, at a given temperature was obtained from data such as those shown in Fig. 2 using

$$S_0^R = \frac{(P_4 - P_2)}{(P_4 - P_1)}. \qquad (2)$$

Summarized in Fig. 3 are measurements of S_0^R as a function of temperature for CD_3OH, CH_3OH, and CH_3OD. Duplicate measurements were made for every CD_3OH and CH_3OD data point, but duplicate data are reported only at 351 K to indicate typical reproducibility. Figure 3 illustrates the existence of a kinetic isotope effect for –OD compared to –OH functionalities for methanol decomposition on a clean Ni(111) surface (*1*). The *ratio* S_0^R(O–H)/S_0^R(O–D) is shown in Table 1.

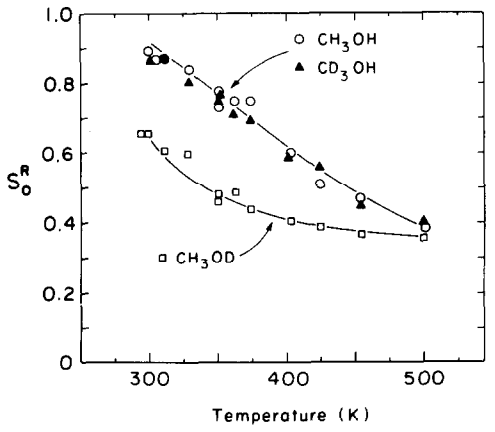

FIG. 3. Plot of zero coverage reactive sticking coefficient, S_0^R, versus temperature for three methanol isotopes. $S_0^R = (P_4 - P_2)/(P_4 - P_1)$, referring to Fig. 2 and to the text. Duplicate data points at 351 K indicate reproducibility.

TABLE 1

Deuterium Isotope Effects in Methanol Decomposition on Ni(111): A Comparison of CH_3OD and CD_3OH

Temperature (K)	$S_0^R(CD_3OH)^a / S_0^R(CH_3OD)$	$\theta_{SS}(CO/CD_3OH)^b / \theta_{SS}(CO/CH_3OH)$	$f_{SS}^R(CD_3OH)^c / f_{SS}^R(CH_3OD)$
301	1.34	1.16	(7.69)
330	1.33	1.15	1.70
351	1.63	1.04	2.04
363	1.45	1.29	2.24
374	1.57	1.50	1.85
400	1.44	0.94	1.84
426	1.44	—	—
450	1.22	—	1.38
500	1.11	—	0.82

[a] Kinetic isotope effect. See Fig. 3.
[b] Concentration isotope effect. See Fig. 8.
[c] Kinetic plus concentration isotope effects. See Fig. 5.

The deuterium kinetic isotope effect for the decomposition of methanol on Ni(111) also exists in the transient region between the beginning of the experiment and the steady-state conditions ultimately achieved. A comparison of the fraction of the methanol flux undergoing reaction, f^R, of the three methanol isotopes is made at 351 K as a function of alcohol exposure in Fig. 4. At a given crystal temperature, the fraction decomposing is evaluated at particular times, t, from data such as those shown in Fig. 2 using

$$f^R = \frac{(P_4 - P_t)}{(P_4 - P_1)}. \tag{3}$$

P_t is the mass spectrometer signal at a given elapsed time, t, for the crystal in the methanol beam. S_0^R and f^R are both dimensionless rate constants.

Figure 4 illustrates that at 351 K, as the surface coverage changes, CH_3OD is consistently less reactive than either CH_3OH or CD_3OH, which have similar reactivity. The data in Fig. 4 also show that f^R is coverage dependent. At 351 K the majority of surface species retained is the methanol decomposition product, CO (see Fig. 8), so that CO(ads) is primarily responsible for the decrease in f^R with exposure.

In the course of an isothermal decomposition experiment, f^R approaches a constant steady-state value for a given molecule and crystal temperature. This limiting value, f_{SS}^R, is the fraction of methanol removed under steady-state conditions. The steady-state condition is characterized by a *constant* CO surface coverage, $\theta_{SS}(CO)$. Since the reflected alcohol signal at the steady-state condition is defined as P_3 (see Fig. 2), the fraction of methanol removed from the beam at steady state is defined by

$$f_{SS}^R = \frac{(P_4 - P_3)}{(P_4 - P_1)}. \tag{4}$$

A deuterium isotope effect is also observed for f_{SS}^R in the temperature range 300 to 500 K. Figure 5 summarizes f_{SS}^R as a function of temperature for three methanol isotopes: CH_3OH, CD_3OH, and CH_3OD. The maximum reaction rate occurs near 375 K. CH_3OH and CD_3OH have greater steady-state reaction rates than CH_3OD. Table 1 summarizes the ratio of the rate constants, f_{SS}^R $(CD_3OH)/f_{SS}^R$ (CH_3OD), which has a value of 1.85 at 374 K and decreases monotonically to approximately unity at 500 K.

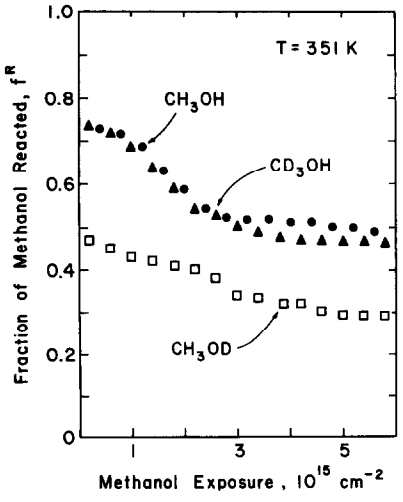

FIG. 4. Plot of fraction of methanol reacted, f^R, versus exposure for three methanol isotopes. $f^R = (P_4 - P_t)/(P_4 - P_1)$, referring to Fig. 2 and to the text. The methanol flux is 2×10^{13} cm^{-2} sec^{-1}.

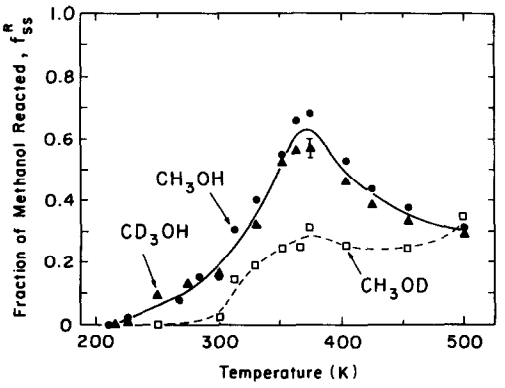

FIG. 5. Plot of the fraction of methanol reacted at steady state, f_{SS}^{R}, versus temperature for three methanol isotopes. $f_{SS}^{R} = (P_4 - P_3)/P_4 - P_1)$, referring to Fig. 2 and to the text. The error bar for CD_3OH at 374 K indicates our measurement reproducibility. The exposure at which P_3 is measured is selected using data of Figs. 6 and 7.

B. CO and H(D) Steady-State Coverages

The steady-state condition is characterized by a *constant* CO surface coverage, $\theta_{SS}(CO)$. This condition is verified by measuring the absolute CO coverage, $\theta_{SS}(CO)$, which is determined by temperature-programmed desorption with the methanol beam on, as described in Section II and shown in Fig. 6. CO coverage measurements are made at various times of exposure of the isothermal Ni(111) crystal to the methanol beam. Typical data are shown in Fig. 6 for an initial Ni(111) temperature of 363 K.

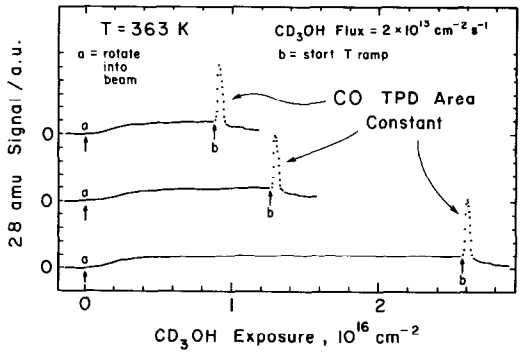

FIG. 6. Representative data showing isothermal production of CO from CD_3OH at 363 K and the subsequent CO thermal desorption peak upon ramping at 2 K/sec. Point (a) indicates the rotation of the crystal into methanol beam. Point (b) indicates the start of the temperature ramp. Constant CO TPD area for three increasing exposures is used to verify the steady-state condition.

In Fig. 7 the buildup of CO coverage to a steady-state condition is shown for CD_3OH and CH_3OD at various crystal temperatures. It is of interest to note from these data that $\theta_{SS}(CO)$ can be measured with high precision. For saturation CO coverage at 363 K, $\theta_{SS}(CO) = 0.24$ for CH_3OD which is 23% lower than for CD_3OH, where $\theta_{SS}(CO) = 0.31$. *Thus, at 363 K the deuterium kinetic isotope effect influences the surface concentration of CO, a stable surface intermediate,* under steady-state conditions.

The temperature dependence of the steady-state absolute CO coverage, $\theta_{SS}(CO)$, for CD_3OH and CH_3OD is presented in Fig. 8. The *relative* steady-state deuterium coverage, $n_{SS}(D)$, for CD_3OH is also shown for qualitative comparison. With increasing temperature, $n_{SS}(D)$ steadily decreases. Below 300 K, it is apparent in Fig. 8 that there is a competition for surface sites between CO and H produced by methanol. As the crystal temperature increases from 250 to 300 K, $\theta_{SS}(CO)$ increases and $n_{SS}(D)$ decreases. A maximum in $\theta_{SS}(CO)$ is observed at 305 K and $\theta_{SS}(CO)$ then decreases to zero above 425 K. $\theta_{SS}(CO)$ from

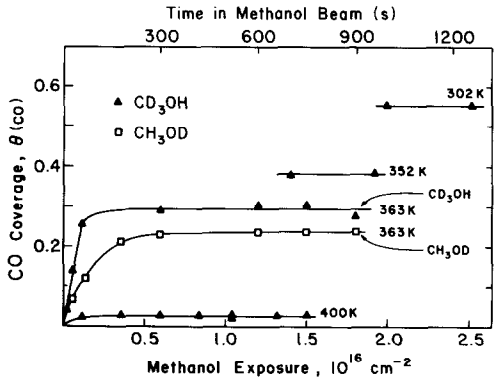

FIG. 7. Plot of CO coverage, θ(CO), versus methanol exposure at several temperatures, showing the attainment of steady-state conditions. Two isotopic methanol molecules are compared at 363 K, illustrating the isotope effect on θ(CO).

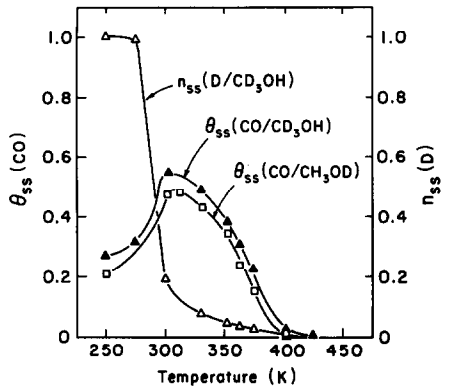

FIG. 8. Plot of steady-state CO absolute coverages, θ_{SS}(CO), versus temperature comparing CD_3OH and CH_3OD. The steady-state D coverage, n_{SS}(D), for CD_3OH is also shown. Determination of absolute CO coverage is described in Section II.

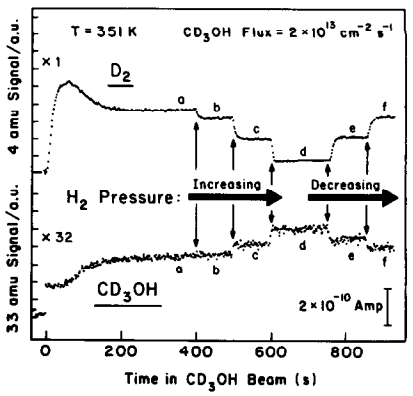

FIG. 9. Representative data showing H_2-controlled isothermal decomposition of methanol on Ni(111) at 351 K. At zero time, rotation of the crystal into the methanol beam occurs. The vertical arrows indicate when the H_2 pressure is changed. The H_2 pressures (a–f) and analysis of these data are listed in Table 2.

CH_3OD follows the same trend as from CD_3OH but is *consistently lower*. Thus, over the temperature range 250 to 425 K we observe that the deuterium kinetic isotope effect influences the steady-state CO surface concentration. Table 1 compares in various ways the isotope effect as a function of temperature. The ratios in Table 1 represent kinetic, concentration, and kinetic plus concentration isotope effects.

C. Product Addition Experiments

Reaction products, CO and H_2, were separately added to the reaction chamber during CD_3OH beam decomposition experiments in order to demonstrate *product inhibition* of the rate of reaction (1). Data from one temperature, 351 K, are presented for product injection experiments. Referring to Fig. 8, at 351 K, the steady-state coverage of CO on the Ni(111) surface is moderately high; a relatively small $D_{(ads)}$ concentration exists under reaction conditions, and as seen in Fig. 5 the steady-state reaction rate at 351 K is about 90% of the maximum. Because of the higher desorption energy for CO compared to H_2, large effects on the decomposition rate are expected due to CO addition at 350 K, with smaller effects expected due to H_2 addition. Product addition experiments are illustrated by Figs. 9 and 10, for H_2 and CO, respectively.

Figure 9 demonstrates control of the

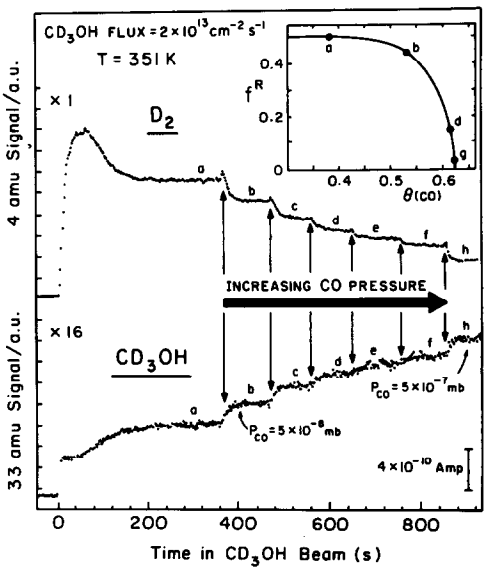

FIG. 10. Representative data showing CO-controlled isothermal decomposition of methanol on Ni(111) at 351 K. At zero time, rotation of crystal into the beam occurs. The vertical arrows indicate when the CO pressure (a–h), is increased. The inset is a plot of the fraction of methanol reacted, f^R, at 351 K versus the coverage of CO, θ(CO), which varies with the CO pressure. The data points of the inset are obtained in separate experiments; see Table 3.

TABLE 2

H_2 Addition Experiment at 351 K[a]: CD_3OH Flux = 2×10^{13} sec^{-1} cm^{-2}

Letter label in Fig. 9	P_{H_2}[b] (mbar)	f^R[c]	$H_2:CD_3OH$ flux ratio[b]	Time for arrival of one monolayer H_2[b] (sec)
a	0	0.58	0:1	—
b	2×10^{-8}	0.56	1.1:1	83
c	2×10^{-7}	0.48	11:1	8.3
d	2×10^{-6}	0.37	110:1	.83
e	2×10^{-7}	0.46	11:1	8.3

[a] Refer to Fig. 9.
[b] Corrected for ion gauge sensitivity.
[c] Rates of reaction (1) in this column are not rigorous steady-state rates, since transient effects are retained to some degree.

CD_3OH decomposition rate using H_2 addition at H_2 pressures of 1×10^{-8} mbar (b), 1×10^{-7} mbar (c, e), and 1×10^{-6} mbar (d). (The corresponding H_2 pressures inside the differentially pumped QMS shield are about 100 times less.) An isothermal CD_3OH beam decomposition is started exactly as in Fig. 2 (right panel), and the system is allowed 400 sec to reach steady state. H_2(g) is then added via a leak valve to give a stable total pressure in the reaction chamber *without affecting the CD_3OH beam flux*. Details of the H_2 addition experiments are summarized in Table 2. A general trend toward reversible behavior is demonstrated upon decreasing the H_2 pressure (intervals e, f). Lack of complete reversibility seen by comparison of c to e and a to f in Fig. 9 and Table 2 is due to the short time intervals used, following each change in H_2 pressure.

Hydrogen desorbs from clean Ni(111) below 350 K (see Fig. 8), and a corresponding weak inhibition effect is seen. An arrival rate (flux) ratio of 110:1 $H_2:CD_3OH$ (see Table 2, (d)) only decreases the fraction of reacting CD_3OH from 0.58 to 0.37, a 36% inhibition effect.

The CO addition experiment of Fig. 10, and related experiments summarized in Table 3, have been analyzed in greater detail than those for H_2 addition. The CO surface coverage during steady-state CD_3OH decomposition was measured *in the presence of added CO*. Each experiment begins exactly as described in Section II. Exposure of the crystal for 350 sec is allowed for achievement of steady state, and CO(g) is then added through the leak valve. As seen in the top panel of Fig. 10, *evolved product* D_2 signal decreases with each increase in CO pressure. Also, a transient CO displace-

TABLE 3

CO Addition Experiments at 350 K[a]: CD_3OH Flux = 2×10^{13} cm^{-2} sec^{-1}

Letter label in Fig. 10	Added CO pressure (mbar)	θ(CO)[b]	f^R[b]	CO:CD_3OH flux ratio[c]	Time for one monolayer[d] CO exposure[c] (sec)
a	0	0.39	0.52	0:1	—
b	5×10^{-8}	0.53	0.45	0.67:1	140
c	1×10^{-7}	—	—	1.3:1	70
d	1.5×10^{-7}	0.62	0.15	2.0:1	47
e	2.0×10^{-7}	—	—	2.7:1	35
f	2.5×10^{-7}	—	—	3.3:1	28
g	3.0×10^{-7}	0.63	0.03	4.0:1	23
h	5×10^{-7}	—	—	6.7:1	14

[a] Refer to Fig. 10.
[b] Measurements from steady-state experiments, separate from Fig. 10. Data not shown.
[c] Corrected for ion gauge sensitivity.
[d] 1.86×10^{15} cm^{-2}.

ment of D_2 from the Ni(111) surface may be seen to different degrees at the beginning of each CO step. The bottom panel of Fig. 10 shows the *reflected reactant* CD_3OH signal increasing with increased CO pressure. A quantitative summary of CO addition experiments appears in Table 3.

The inset to Fig. 10 conveys the key result of our CO addition experiments. *Inhibition of reaction* (1) *by product CO occurs because CO occupies surface sites, blocking methanol adsorption.* At 351 K, a 6.7:1 $CO:CD_3OH$ ratio of arrival rates results in greater than 94% inhibition of the rate of reaction (1) (see h, Table 3 and Fig. 10). This rate inhibition must occur due to CO adsorption because the D(H) surface coverage is very low at 351 K. Similar CO injection results have been observed at 330, 365, and 375 K but the effect is most dramatic at 351 K.

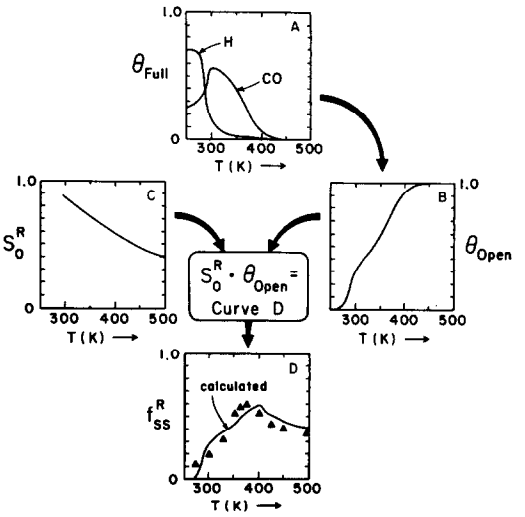

FIG. 11. Schematic construction of the kinetic model using the fraction of empty surface sites (θ_{open}) and the zero coverage sticking coefficient (S_0^R) for CD_3OH. A and C are redrawn from Figs. 8 and 3, respectively. B is derived from A by subtraction: $\theta_{open} = 1 - [\theta(CO) + \theta(H)]$. $\theta(H)$ is estimated as 0.7 times $n_{SS}(D)$ (see Fig. 8 and text). D compares the product ($S_0^R \cdot \theta_{open}$), solid line, with CD_3OH steady-state rate data of Fig. 5, solid triangles.

IV. DISCUSSION

A simple model based on the concept of site blocking readily explains the observed temperature dependence of the rate of reaction (1). Figure 11 illustrates our construction of this site blocking model, and summarizes our kinetic studies of CD_3OH decomposition on Ni(111).

Figure 11A is redrawn from Fig. 8, showing CO and D atom surface coverage under steady-state conditions versus temperature. CO coverage, $\theta(CO)$, is expressed in absolute terms (CO per Ni atom). The relative D atom coverage (Fig. 8) has been multiplied by 0.7 to obtain an empirical value of $\theta(H)$ which optimizes the agreement between the model and our decomposition rate data. Figure 11B is derived from A by subtraction. Figure 11B shows the temperature dependence of the fraction of *empty* surface sites, θ_{open}. The S_0^R versus temperature curve of Fig. 11C is redrawn from Fig. 3, showing the *decrease* in *zero coverage* reactive sticking probability with increasing temperature for CD_3OH. The ordinate of Fig. 11D is the *product* $S_0^R \cdot \theta_{open}$, or the fractional probability of successful CD_3OH reaction on the surface *under steady-state conditions*. The solid line of Fig. 11D indicates the behavior of $S_0^R \cdot \theta_{open}$. This is compared with our data points (solid triangles) from Fig. 5 for the rate of reaction (1) under steady-state conditions.

Figure 11 shows that above 400 K, the fraction of empty sites rapidly approaches unity (Fig. 11B) and the rate of reaction (1) is proportional to S_0^R. From 300 to 375 K, the fraction of empty sites approximately doubles (Fig. 11B), while S_0^R decreases by only 15–20% (Fig. 11C). Therefore, the opening up of empty surface sites is the dominant factor controlling the rate of methanol decomposition below 375 K. Above about 400 K, the decline in the reactive sticking coefficient for methanol on open sites is the dominant factor controlling the fall off in decomposition rate. *We describe the dominant factors controlling the kinetics of reaction (1) below 375 K as site*

blocking by adsorbed products, and *above 375 K as methanol dissociation to methoxy and surface H atoms.*

Referring to Table 1, CH_3OD is characterized by a purely *kinetic* isotope effect in S_0^R, and a deuterium isotope effect in f_{SS}^R, which may have both kinetic and concentration contributions. Table 1 and Figs. 7 and 8 emphasize that the concentration of a stable surface intermediate (such as CO) also is influenced by a deuterium isotope effect. A *detailed* interpretation of the O–H versus O–D isotope effect is only possible on the clean surface from the ratio of S_0^R(O–H)/S_0^R(O–D) which is known to be of purely *kinetic* origin (*1*).

As emphasized in Figs. 3, 4, and 5, CD_3OH and CH_3OH exhibit the same reaction probability under zero coverage (Fig. 3), transitory (Fig. 4), and steady state conditions (Fig. 5). The absence of a kinetic isotope effect for C–D versus C–H in methanol decomposition via a methoxy intermediate indicates that the rate determining step (r.d.s.) *must precede* C–H (C–D) bond scission. We therefore believe that the elementary step leading to methoxy *formation* is the r.d.s. in the decomposition reaction (1) under both clean surface and steady-state conditions. The similarity of the magnitudes of the KIE observed for S_0^R and for the overall rate of the decomposition reaction, f_{SS}^R (see Table 1) also supports methoxy formation as rate determining under steady-state conditions.

Decomposition is rapid, compared to formation, for methoxy on Ni(111) from 300 to 500 K. Richter, Ho, and co-workers have recently studied methanol decomposition on Ni(110) using a unique time-resolved electron energy loss (TREELS) spectrometer (*9*). They observe methoxy decomposition at 290 K for high methoxy coverage on the (110) surface, and at 270 K for low coverage conditions (*9*). Recombination of methoxy to methanol is observed at 290 K by us (*10*) in temperature-programmed experiments on the Ni(111) surface when methoxy coverage is high. Observations of *stable* CH_3O/Ni(111) around 200 K (*11, 12*), and rapid methoxy decomposition at 290 K and above (*9, 10,* and this work) enable an inference to be drawn. The methoxy decomposition step must have a high activation energy (large temperature dependence), enabling a slow step at $T < 290$ K to become rapid above 290 K.

The competition between CO and H for surface sites seen in Fig. 8 below 300 K (i.e., below the *threshold* for H_2 thermal desorption) is justified on thermodynamic grounds. Isosteric heats of adsorption are 63 kcal/mole for H/Ni(111) (*13*) and 27 kcal/mole for CO/Ni(111) (*7*).

We are able to measure S_0^R and the coverage of stable intermediates, *and* the steady-state rate all in a *single* experiment at any selected temperature. The qualitative success of a site blocking model, involving S_0^R and θ_{open} as input parameters, to describe the kinetics of reaction (1) underscores the utility of this experimental method.

V. SUMMARY

An apparatus and methodology have been presented for the detailed kinetic analysis of surface-catalyzed reaction rates observed in low flux (10^{12}–10^{14} cm^{-2} sec^{-1}) flow reactions over single crystal catalysts. We have reached a quantitative understanding of the rate versus temperature behavior for the net reaction

$$CH_3OH(g) \xrightarrow{Ni(111)} CO(g) + 2H_2(g) \quad (5)$$

using this method.

The following important quantities are measured in *one isothermal experiment:*

(1) steady-state reaction rate,

(2) surface coverage of stable intermediates,

(3) zero coverage reactive sticking coefficient.

Detailed insight into the mechanism of the above reaction has emerged, including these observations:

(A) The steady-state rate of reaction (1) has been measured as a function of temper-

ature from 200 to 500 K for CH_3OH, CD_3OH and CH_3OD.

(B) A deuterium kinetic isotope effect has been used to *identify* the O–H bond as the initial *reactive center* in CH_3OH chemisorption from 290 to 500 K. An unstable CH_3O intermediate is thus identified.

(C) The isotope effect on the methanol decomposition rate has also been observed under steady-state conditions. Here isotopic factors also play a role in governing steady-state surface coverages.

(D) Product inhibition of reaction (1) by CO(ads) and H(ads) occurs via site blocking.

(E) A site blocking model accurately describes the steady-state decomposition rate as a function of temperature. The parameters used in the site blocking model are all *simultaneously* measured with our method.

ACKNOWLEDGMENT

The authors gratefully acknowledge full support of this work from the Army Research Office through Contract DAAG29-83-K-0141.

REFERENCES

1. Gates, S. M., Russell, J. N., Jr., and Yates, J. T., Jr., *Surface Sci.* **146,** 199 (1984).
2. Goodman, D. W., Kelley, R. D., Madey, T. E., and Yates, J. T., Jr., *J. Catal.* **63,** 226 (1980).
3. Goodman, D. W., *J. Vac. Sci. Technol.* **20,** 522 (1982).
4. Somorjai, G. A., "Chemistry in Two Dimensions: Surfaces." Cornell Univ. Press, Ithaca, N.Y., 1981.
5. Madix, R. J., Benziger, J., *Annu. Rev. Phys. Chem.* **29,** 285 (1978); Madix, R. J., *in* "Chemistry and Physics of Solid Surfaces" (R. Vanselow, Ed.), Vol. II. CRC Press, Boca Raton, Fla., 1979.
6. Ertl, G., *Catal. Rev. Sci. Eng.* **21,** 201 (1980); Ertl, G., *J. Vac. Sci. Technol. A* **1,** 1247 (1983).
7. Christmann, K., Schober, O., and Ertl, G., *J. Chem. Phys.* **60,** 4719 (1974).
8. Netzer, F. P., and Madey, T. E., *J. Chem. Phys.* **76,** 710 (1982).
9. Richter, L. J., Gurney, B. A., Villarrubia, J. S., and Ho, W., *Chem. Phys. Lett.*, in press.
10. Gates, S. M., Russell, J. N., Jr., and Yates, J. T., Jr., *Surface Sci.*, submitted.
11. Demuth, J. E., and Ibach, H., *Chem. Phys. Lett.* **60,** 395 (1979).
12. Erskine, J. L., and Bradshaw, A. M., *Chem. Phys. Lett.* **72,** 260 (1980).
13. Christmann, K., Schober, O., Ertl, G., and Neumann, M., *J. Chem. Phys.* **60,** 4528 (1974).